Production of metastable negative ions in a cesium sputter source: Verification of the existence of N_2^- and CO^-

Roy Middleton* and Jeff Klein
Department of Physics and Astronomy, University of Pennsylvania, 209 South 33rd Street, Philadelphia, Pennsylvania 19104-6396
(Received 15 October 1996; revised manuscript received 22 April 1998)

We present a study of the production of metastable negative ions by cesium sputter sources. We report measurements of relatively intense (~0.5 nA) beams of N_2^- and CO^-, two ions with extremely low (<-2.3 eV) electron affinities, and show that they form metastable negative ions with comparatively long lifetimes. Surprisingly, the current of N_2^- is comparable in intensity to N_3^-, a molecular negative ion with a binding energy of 2.8 eV. The existence of metastable N_2^- has a twofold significance. First, N_2^- may play an important role in atmospheric chemistry. Second, N_2^- is an excellent test of calculations on many-body systems involving electron-correlation effects. We verified the identification of the ions discussed in this paper using the techniques of accelerator mass spectrometry and Coulomb-explosion imaging. Using an in-beam decay technique, we determined lower bounds for the lifetimes of the most stable states of N_2^-, CO^-, and CO_2^-: 180 ± 30, 140 ± 25, and 170 ± 30 μs, respectively. We also report intensities of Be^- and beryllium cluster negative ions, Be_n^-, for $n=2-6$. [S1050-2947(99)07205-4]

PACS number(s): 79.20.Rf, 36.40.Wa, 41.75.Cn, 39.10.+j

I. INTRODUCTION

The known metastable negative ions are built on excited states of neutral atoms, i.e., excitations of core electrons, where the negative ion is stabilized because its direct decay to the ground state is forbidden. Usually the neutral excited state on which the negative ion is built lies several eV above the ground state. As examples, consider He in which the $(1s^1 2s^1)^3S$ state lies 19.8193 eV above $(1s^2)^1S^0$ ground state, and Be where the $(1s^2 2s^1 2p^1)^3P^0$ state lies 2.7253 eV [1–3] above the $(1s^2 2s^2)^1S^0$ state. The negative ion is only weakly bound with respect to the excited state [He^- is bound by 77.518 ± 0.011 meV (theoretical) and 77.516 ± 0.006 meV (experimental) [4], Be^- is bound by 289.10 ± 1.0 meV (theoretical) [5], and 290.99 ± 0.10 meV [6] (experimental)]. For He and Be, the negative ions are constructed by adding an electron with parallel spin to the triplet state of the core-excited neutral to form $(1s^1 2s^1 2p^1)^4P^0$ in the case of He^-, and $(1s^2 2s^1 2p^2)^4P^0$ in the case of Be^-. The spin-stabilized quartet state cannot decay easily to the ground state. The usual decay mode is by relativistic Coulomb excitation [7,8]. The lifetimes of these quartet negative ions are typically in the range of 10^{-5} s, which is much longer than the lifetimes of the negative ions built on the ground state of the neutral atom. Corresponding ground-state-based negative ions for these atoms have lifetimes on the order of the vibrational period, $10^{-16}-10^{-15}$ s. Conceptually, one imagines making metastable negative ions in two steps: In the first step, a neutral atom in the ground state is excited by a few (2–30) eV to produce a triplet neutral atom; and in the second, an electron with parallel spin is attached to form the metastable quartet state.

Although the constructional details of all metastable ions are not identical, it is probably a fair guess that all metastable ions are spin stabilized. For molecular ions, additional factors may also contribute to stability. Conformational stabilization (Franck-Condon effect) can be significant when a negative ion differs in shape or size from the neutral molecule. When spatial differences are significant, the overlap of the wave functions of the ion and molecule is small, thereby reducing the chance of vertical autoionization (i.e., loss of electron without motion of the atomic nuclei). CO_2^- is a case in point: CO_2^- is bent, but CO_2 is linear. Differences in bond lengths in N_2 and N_2^- may help to stabilize N_2^-. Molecules also have many more modes over which to partition energy than do atoms—dividing excitation energy over these additional modes can contribute to the stability of a negative ion, often by helping to get rid of excess energy produced during electron attachment to the molecule.

Metastable negative ions are produced customarily by charge exchange, in part because it is generally believed that metastable negative ions are formed only weakly in sputter sources. But the evidence supporting this belief is weak. Only one published paper compares the currents of a metastable negative ion produced in a sputter source to the currents achievable through charge exchange. Although Kutschera *et al.* [9] reported that He^- currents from sputter sources are several orders of magnitude less than from charge exchange, the poor yield of He^- from the source used by Kutschera *et al.* may have an alternative explanation. To produce He^-, they sprayed helium gas onto a titanium surface, with the idea that the high chemical reactivity of titanium would allow it to getter the He long enough that the He could be sputtered by incident Cs ions. The approach yields prolific currents for comparatively reactive gases such as hydrogen and oxygen, but the alternative explanation for the low yield of He^- is that the noble nature of helium prevents it from sticking long enough to the surface to be efficiently sputtered by the Cs.

In high-intensity cesium-sputter sources [10,11], particularly those with spherical ionizers [12,13], the Cs^+ beam is

*Electronic address: jklein@dept.physics.upenn.edu

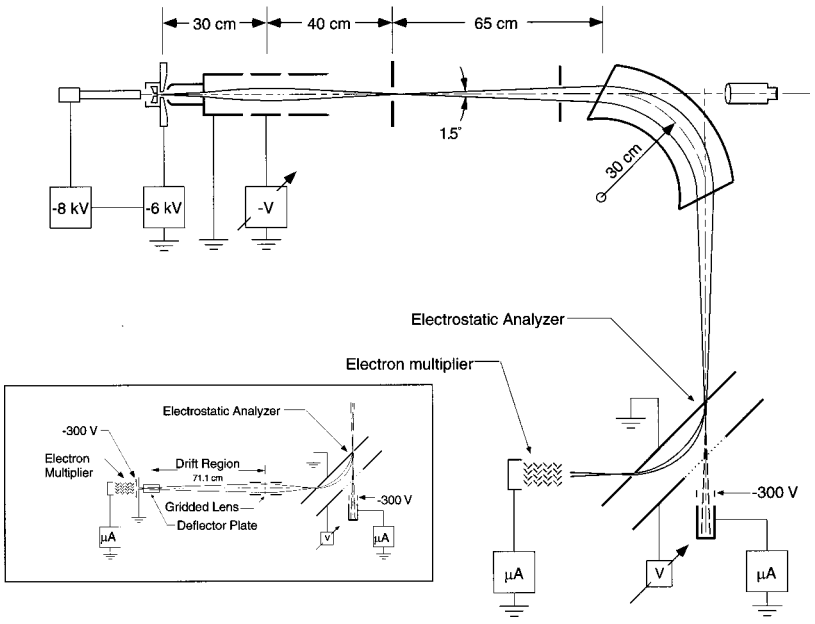

FIG. 1. Modified ion-source test facility and electrostatic analyzer used to make many of the measurements reported here. With narrow slits ($\sim\pm 0.25$ mm) the resolution of the magnetic analyzer ($\Delta m/m$) is about one in 300, and that of the electrostatic analyzer ($\Delta E/E$) about one in 100. The output of the low-gain electron multiplier is connected to a logarithmic amplifier (10^{-4}–10^{-12} A) that in turn drives a chart recorder. The boxed figure shows a schematic of the apparatus that was added to measure lifetimes of metastable ions.

extremely well focused, and rapidly forms a cavity in the sputter target that is small in diameter but deep. As the cavity deepens, an intense and exceedingly small ball of plasma frequently forms, the appearance of which usually coincides with the maximum output of negative ions. The plasma consists of a mixture of atoms and ions of cesium and the target material. For many substances, this plasma is the primary source of negative ions. Sputtered atoms and molecules in various states of excitation traverse the plasma several times before escaping as a neutral atom or being forcibly removed as a negative ion by the extraction electric field. Comparatively long confinement times in the plasma may make sputter sources competitive with charge-exchange sources in forming metastable negative ions. Recognition of this possibility motivated the present study.

II. EXPERIMENTAL PROCEDURE

The investigations we report were usually initiated on our modified ion-source test facility and completed on our FN tandem accelerator. The test facility is essentially a moderately high-resolution ($\Delta M/M\sim 1/300$) mass spectrometer that consists of a high-intensity source with a spherical ionizer, a double-focusing 30-cm-radius 90° magnet, and a 90° electrostatic analyzer—see Fig. 1.

The high-intensity cesium-sputter source is similar to that described in Refs. [12, 13]. Figure 2 shows the main components of the source: a liquid-cooled cathode that can be changed without breaking the vacuum, a spherical molybdenum ionizer that operates at a temperature of $\sim$1100 °C, a cesium spray system that also serves as an electrode that helps to optimize the focus of the Cs^+ ions on the cathode, and an extract electrode. Measurements were made with the cathode at a negative potential of 38 kV, the ionizer at 30 kV, and the extract electrode at ground potential. The current between the ionizer and the cathode was typically 4–5 mA—about 1 mA due to Cs^+ ions and the remainder to electrons. The open structure of this source compared with that used in the earlier high-intensity sources that employed a helical ionizer [10,11] results in appreciably improved vacuum in the negative-ion formation region ($\sim 10^{-7}$ Torr), and less neutralization on account of collisions. Atomic and molecular negative ion currents vary widely depending on the electron affinity of the sputter target and the physical properties affecting sputtering. In favorable cases currents in excess of 100 μA are common, while in less favorable cases currents may be as low as 10 nA.

The electrostatic analyzer (ESA), which consists of two flat parallel metal plates that produce a uniform electric field, has a resolution of $\Delta E/E\sim 1/100$ with the entrance and exit slits at ± 0.25 mm. The analyzer is located after the magnet (see Fig. 1), and a gridded aperture in its back plate allows ions to pass through it and into a Faraday cup when the electric field in the analyzer is off. With the field on, ions are deflected through 90°, and exit the analyzer through a second slit in the grounded front plate into an electron multiplier. The electron multiplier was chosen for ruggedness, and can measure incident currents up to 10 μA with a gain of up to 1000. The current from the multiplier is read by a Keithley 2600 loga-

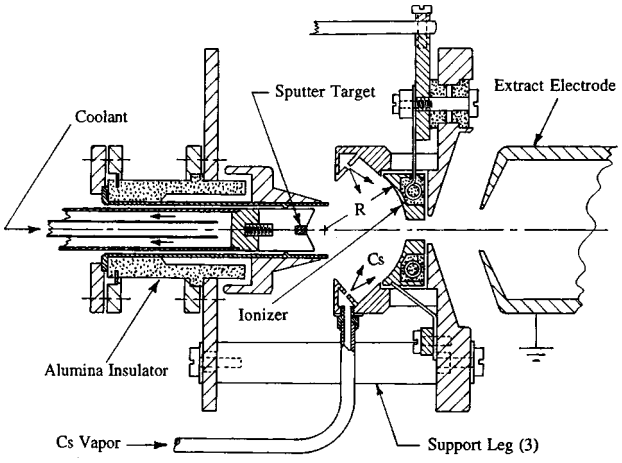

FIG. 2. Latest version of our high-intensity ion source as used to make the measurements reported here. Basically identical sources are used on the ion-source test facility and on the tandem accelerator.

rithmic meter covering the range 10^{-12}–10^{-4} A. Currents as low as 10^{-15} A can be measured, and currents as low as 10^{-16} A detected. Spectra are recorded on a chart recorder.

A major difficulty in mass spectrometry is resolving isobaric ambiguities. For example, a resolution $(\Delta M/M)$ of at least one in 10^3 is required to distinguish between $^{28}Si^-$ and $^{14}N_2^-$; if there is a large disparity in intensities, a resolution of 10^4 or larger may be necessary. A tandem accelerator, particularly one instrumented for accelerator mass spectrometry (AMS), provides an alternative means of isobaric identification since it provides a means of eliminating all molecular interferences and identifying the Z of all atomic ions. Recently, we used our tandem and AMS beam line to positively identify doubly-negative carbon clusters consisting of seven or more atoms [14], and, even more recently [15], to identify the molecular dianions BeF_4^{2-} and MgF_4^{2-}. These and closely related techniques were used to identify and confirm the existence of the anions reported here.

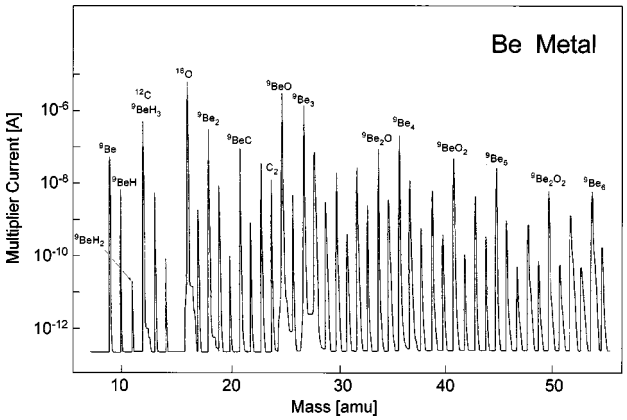

FIG. 3. Typical spectrum from a cathode prepared from high-purity beryllium metal. The identities of many of the peaks were verified by acceleration through our FN tandem. Note that $^9Be^-$ is formed with remarkable intensity (see the table in the text), in spite of its being a metastable ion.

III. EXPERIMENTAL RESULTS

A. Beryllium (Be_n^-)

The ground-state negative ion of beryllium is unbound, but a metastable negative ion first observed by Bethge, Heinicke, and Baumann [16] and theoretically investigated by Weiss in 1968 [17], can be built from an excited triplet of the neutral atom formed by promoting a $2s$ electron to a $2p$ orbital. Although this excited state lies 2.723 ± 0.007 eV [3] above the ground state; it is nearly stable to electromagnetic decay, because decay to the ground state requires a spin flip as well as change in angular momentum of one unit. Its decay mode is by relativistic autoionization. The negative ion is made by adding another electron with parallel spin to the $2p$ orbital, so the configuration of the negative ion is $(1s^2 2s 2p^2)^4P$. This state has been measured recently to lie 290.99 ± 0.10 meV [6] (in reasonable agreement with the earlier two measurements [3,18]) below the triplet excited state, and hence is bound. Recent calculations [5] yielding 289.10 ± 1.0 meV for the binding energy are in very good agreement with this measured value, though earlier calculations have yielded a range of values from 190 ± 110 to 285 meV [17,19,20]. Much progress has been made recently on measuring the lifetime of Be^-. A long-lived, fine-structure, component of the ^4P state with a lifetime of 45 ± 5 μs was reported by Balling *et al.* [21] based on a storage-ring experiment. Identification of this state with the $^4P_{3/2}$ component is based on theory, and its long lifetime is attributed to the destructive interference of the direct relativistic and relativistically induced Coulomb detachment [22]. In a subsequent measurement using resonant two-photon detachment combined with resonant-ionization detection of the neutral atoms, Anderson *et al.* [23] measured the lifetimes of the $^4P_{1/2}(0.73 \pm 0.08\ \mu s)$ and $^4P_{5/2}(0.33 \pm 0.06\ \mu s)$ levels. These latest measurements are in good agreement with the latest theoretical predictions [24], even though they are about two orders of magnitude shorter than previous calculations [22,25].

The beryllium metastable negative ion is nearly an exact analog of He^-, and consequently seemed a good ion to test our hypothesis that the poor yield of He^- from sputter sources was due to low chemical reactivity and short residence time on the cathode and not because sputter sources have difficulty forming metastable ions.

A beryllium cathode was prepared by pressing a 6-mm-diameter piece of high-purity beryllium metal rod into one our standard copper cathodes. The first measurements with this cathode were made on our test facility, and Fig. 3 shows a typical spectrum. The relative intensities in Fig. 3 are approximate, because the response of the electron multiplier is somewhat nonlinear for molecular ions, where the simultaneous arrival of several atoms can cause saturation of the dynodes. Not only is $^9Be^-$ evident in the spectrum, but it is also accompanied by several homonuclear cluster ions, the most intense being the trimer.

A second identical cathode was studied using the tandem injector and the identities of the uncertain peaks were checked by acceleration. Unlike the test facility where the beam is highly collimated by very narrow slits, the apertures and slits on the injector are no smaller than required for good transmission, so that the negative-ion currents measured in the low-energy Faraday cup are much more meaningful. Table I lists the intensities of the first six homonuclear polyatomic ions of beryllium. As is evident from the table, the metastable atomic anion is reasonably intense, and its yield is comparable to that of many metals with electron affinities in the range 0.1–0.25 eV forming stable anions. We conclude that Be_2^- is definitely metastable with a lifetime >180 μs, while Be_3^- is either stable or has a lifetime of >500 μs.

B. Nitrogen dimer (N_2^-)

The negative ions of nitrogen present an enigma. There is a wealth of theoretical [19,26,27] and experimental evidence [27–31], that, while often conflicting, generally concurs that

TABLE I. Relative intensities of the negative ions of beryllium clusters.

Ion	Be^-	Be_2^-	Be_3^-	Be_4^-	Be_5^-	Be_6^-
I^- (μA)	0.45	0.67	2.9	0.19	0.025	0.029

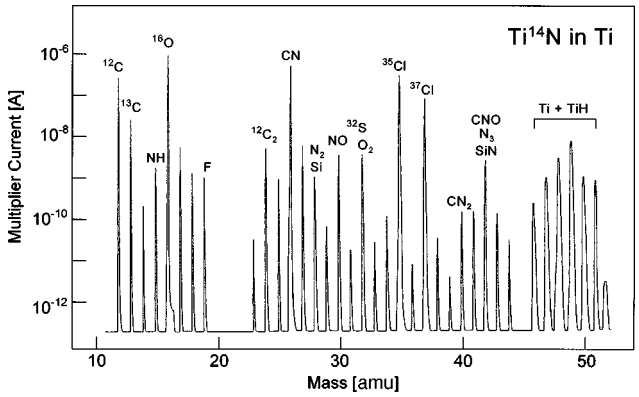

FIG. 4. A spectrum measured with the system shown in Fig. 1 with a titanium metal cathode containing titanium nitride tamped into a 2-mm-diameter hole. Of particular interest are the peaks at mass 28 and 42, that were established to be due in part to N_2^- and N_3^- ions (see text).

N^- is unstable in its ground state. However, a metastable negative-ion with a lifetime much shorter than 1 μs (<200 ns is currently the best estimate [28]) probably exists. Indeed, it is the instability of N^- that enables the widespread use of tandem accelerators for radiocarbon dating. Massey [32], in his well-known monograph on negative ions, presents compelling theoretical arguments that the dimer N_2^- is also unstable in its ground state, despite the earlier evidence from low-energy electron-scattering data [33] and subsequent studies that showed evidence of a strong (though broad and presumably short lived) resonance between 1.8 and 3.8 eV, which could very well imply the existence of a metastable state. Experimental evidence supporting the instability of N_2^- was obtained in Ref. [31]. Scheller, Compton, and Cederbaum [34], in a recent review article, reported an electron affinity of about -2.6 eV (that is presumably based on the low-energy scattering data). The N_3^- trimer ion was first observed in Ref. [35], and its electron affinity first measured directly in Ref. [36] using an ion cyclotron resonance spectrometer. From photodetachment measurements, the latter authors determined the electron affinity of N_3^- to be 2.70 ± 0.12 eV. More recent measurements by Illenberger *et al.* [37] now place this value at 2.76 ± 0.04 eV.

1. Experimental results

In this section we present evidence from five experiments that independently prove the existence of N_2^-. For any less contentious ion, any one of these results on its own would have been proof enough. Taken in sum, we believe that they provide incontrovertible evidence for the existence of N_2^-.

To provide a perspective of the evidence we adduce for the existence of N_2^-, we first summarize the results of our measurements and then subsequently provide the experimental details. Initial spectra obtained using the ion-source test facility with a cathode of $Ti^{14}N$ showed peaks at masses 28 and 42 (see Fig. 4) that we suspected were N_2^- and N_3^-, but a lack of sufficient resolution prevented us from ruling out $^{28}Si^-$, $^{12}C_2H_4^-$, $^{13}C_2H_2^-$, etc. as the cause of the peak at mass 28, or $^{28}SiN^-$ or another molecular ion other than N_3^- at mass 42. To establish the identities of these peaks, we made a series of measurements on the tandem accelerator.

(1) Using a cathode containing roughly equal parts of Ti ^{14}N and Ti ^{15}N, we analyzed beams of $^{14}N^{3+}$ and $^{15}N^{3+}$ while injecting negative ions of mass 28, 29, and 30. The 3+ charge state was chosen to ensure that the measured beams were atomic and not molecular. Above charge state 2+ nearly all molecular ions are unstable [38], and are consequently destroyed in the stripper. Thus, while analyzing $^{14}N^{3+}$, the only significant interfering beam is $^{28}Si^{6+}$ which differs sufficiently in mass to be resolved by the high-energy magnet. The strongest support for the existence of N_2^- from this set of measurements was the equality of the $^{14}N^{3+}$ and $^{15}N^{3+}$ beams when mass 29 ions were injected (implying that the injected ion at mass 29 was $^{14}N\,^{15}N^-$).

(2) Switching to a gas cathode, we show that the measured current of $^{14}N^{3+}$ was proportional to the partial pressure of N_2 in the source, and that the $^{28}Si^{6+}$ current actually decreased as the pressure of N_2 increased. These observations confirmed the identification of the analyzed beams of $^{28}Si^{6+}$ and $^{14}N^{3+}$ (which were not in doubt in the first place since these beams peak at terminal voltages that are different by $\sim$6 kV at 6 MV).

(3) Using a technique we developed to study molecular dianions [14], we show that the beam of $^{14}N^{3+}$ ions analyzed when injecting negative ions with mass 28 into the accelerator actually consists of pairs of nitrogen ions, and, when injecting mass 42, triplets of ions. These measurements were made with an ionization detector capable of determining the energy and nuclear charge (Z) of single ions. In addition to being able to determine the multiplicity of the incoming ions, we were able to verify that the detected ions had $Z=7$ and an energy of 21 MeV, as expected for $^{14}N^{3+}$.

(4) We used the Coulomb-explosion technique to image the molecules accelerated to the terminal of the tandem. The images were dominated by diatomic homonuclear molecules when the injection magnet was set to mass 28. We observed a few tracks made by atoms of higher Z that we believe are $^{28}Si^-$ ions that were not completely eliminated by the negative-ion injector (where the mass resolution is about 1/300). The Coulomb-explosion images rule out larger molecules (containing more than two atoms) as the source of the two nitrogen ions we observe in (3) above. The plastic detector would have detected protons had they been present, eliminating the possibility of hydride contamination in the injected beam.

(5) Using the ion-source test facility, we measured the lifetime of N_2^- to be 180 ± 30 μs, suggesting (1) that N_2^- is metastable, and (2) that its lifetime is amply long enough to permit its acceleration through the tandem.

2. Experimental details

(a) Identification of N_2^-. We began investigating N_2^- using our ion-source test facility with a cathode made by packing titanium nitride (Ti ^{14}N) into a 1.6-mm-diameter hole in a titanium metal cathode. Figure 4 shows a typical spectrum. As expected, moderately intense peaks were observed of $^{14}NH^-$ and C $^{14}N^-$, and a peak at mass 30 was tentatively identified as $^{14}N\,^{16}O^-$. The peak at mass 14 is a combination of $^{12}CH_2^-$ and $^{13}CH^-$ and not $^{14}N^-$. Peaks of nearly equal intensity were observed at masses 28 and 42, at the positions expected for $^{14}N_2^-$ and $^{14}N_3^-$, respectively. However, even though we determined that the peak at mass

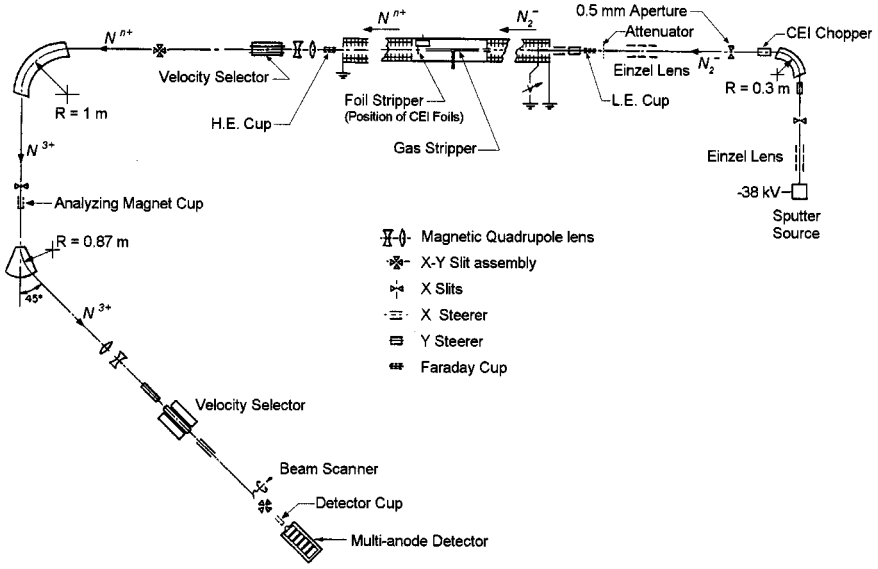

FIG. 5. Layout of the FN tandem accelerator. Negative ions produced in the Cs sputter source, on the right-hand side of the figure, are mass analyzed before injection into the accelerator. The negative ions are accelerated to the central terminal of the tandem, where the gas and/or foil stripper converts them to positive ions. The positive ions are then accelerated back to ground potential. The total energy of the positive ion is $nV_T + m^+/m^-(V_T + V_S)$, where V_T is the terminal voltage (2–10 MV), V_S is the source voltage (38 kV), m^+ is the mass of the positive ion (atom), m^- is the mass of the negative ion (molecule), and n is the charge state of the positive ion. The positive ions are mass and energy analyzed by the combination of magnets and lenses comprising the high-energy transport system. The positive ions for this experiment were detected in the ''analyzing magnet cup,'' the ''detector cup,'' or the ''multianode detector.'' For most measurements, neither velocity selector was employed. Only during the identification and elimination of the $^{14}N^{3+}$ and $^{16}O^{3+}$ peaks observed while injecting mass 30 ions was the velocity selector immediately following the accelerator used. Ion species at various locations while accelerating N_2^- are shown.

28 was a doublet, we could not ascertain how much of the peak was due to $^{28}Si^-$, a common contaminant and a prolific negative ion, and how much to N_2^-. At mass 42, we were unable to resolve N_3^- from $^{28}SiN^-$ or CNO^-.

Because of the interference caused by silicon, a cathode was prepared containing almost equal parts of Ti ^{14}N and Ti ^{15}N.[1] The powders were thoroughly mixed and compressed into a hole in a titanium cathode, as previously described. The cathode was introduced into the tandem's high-intensity Cs sputter source (essentially identical to the source on the ion-source test facility). The sample was sputtered with 8-keV Cs^+ ions, and the source was operated with an extraction voltage of 30 KeV, producing ions with a total energy of 38 keV. These ions were mass analyzed by the tandem's 90°, double-focusing, 30-cm-radius, injection magnet (see Fig. 5). The object slits and the image aperture of the magnet were set to ± 0.25 mm (except when the object slits were closed essentially to zero to attenuate the beam, see below). Under these conditions, mass 29 negative ions were selected with a mass resolution of $M/\Delta M = 300$ and injected into the accelerator. We made a series of measurements at a constant terminal voltage of 6 MV, and used a gas stripper to reduce the Coulomb explosion that occurs when accelerating molecular ions. ''Coulomb explosion'' is the term given to the intense electrostatic repulsion between atomic ions that occurs when the atomic fragments produced by breaking molecular bonds are ionized before the fragments have time to move very far apart. In a foil stripper (with a typical thickness of only ~150 Å), stripping of atomic electrons occurs when the atoms are about one angstrom apart and the Coulomb repulsion between the positively charged atomic fragments is large enough to seriously deteriorate the optics of the high-energy beam. Because of the lower density and longer length (typically ~1 m long) of a gas stripper, the breaking of the molecular bonds and the ionization of the atomic fragments are normally well separated spatially, so the atomic fragments have time to drift apart before they become significantly charged. Use of a gas stripper results in much higher transmission and smaller beam size (typically <1-mm diameter for positive ions at the high-energy end of our accelerator) when negative molecular ions are injected. With the terminal at 6-MV 20.915-MeV $^{14}N^{3+}$ ions, 21.123-MeV $^{15}N^{3+}$ ions, and 42.038-MeV $^{29}Si^{6+}$ ions were successively analyzed by readjusting the NMR-controlled high-energy magnet, adjustable with a precision of ~1 ppm. The analyzed currents of $^{14}N^{3+}$ and $^{15}N^{3+}$ were 165 and 155 pA (electrical), respectively, but a slight adjustment of the high-energy quadrupole lens increased the $^{15}N^{3+}$ current to 164 pA—confirming that the currents were essentially equal as they should be if they originated from $^{14}N\,^{15}N^-$. The $^{29}Si^{6+}$ current was 740 pA. We estimate that with a cathode containing 100% Ti ^{14}N the $^{14}N_2^-$ current would be about 1 nA (165 pA × 2 × 7/3, where the factor of 2 is because the cath-

[1]The Ti ^{15}N was prepared by heating titanium powder on a molybdenum substrate in a ^{15}N atmosphere. Conversion is readily visible since the reaction is highly exothermic.

ode we used contained about 50% Ti ^{15}N; the factor of 7 comes from the transmission through the accelerator, about 15% and the factor of one-third because we measured the current of 3+ ions).

This measurement provides strong evidence for the existence of relatively long-lived ($>10\,\mu$s) N_2^- ions. The lifetime estimate is based on the time ($\sim 12\ \mu$s) it takes for an ion to travel from the ion source to the base of the accelerator (a drift length of $\sim$6 m) and from there to the terminal (center) of the tandem (just over 5 m through a potential gradient at 6 MV of $\sim$1.2 MV/m), where it is converted from a negative ion to a positive ion.

To confirm the identification of N_2^- ions, we employed the method used earlier to identify C_n^{2-} ions [14]. We injected mass 28 and 30 ions into the tandem and used our multianode ionization detector [39] to look for coincidences of two $^{14}N^{3+}$ or two $^{15}N^{3+}$ ions, respectively.

We used C $^{14}N^-$ to set up the high-energy transport system (see Fig. 5). The two magnetic dipoles (a 90°, double-focusing, 1-m-radius magnet with a resolution of $M/\Delta M \sim 1600$, and a smaller ''switching'' magnet that deflects through 45°) and two magnetic quadrupoles were adjusted to transport 21.019-MeV $^{14}N^{3+}$ ions into a Faraday cup immediately in front of the detector. The terminal voltage, as indicated by our precision generating voltmeter, was 5.934 MV. Then we attenuated the beam using a 5% transmission plate before the accelerator and by closing the source-magnet object slits until they were essentially touching to achieve a count rate in the detector of $\sim$1 kHz. The beam was admitted into the detector to provide a calibration for the E and ΔE signals characteristic of 21.019-MeV $^{14}N^{3+}$ ions. Once calibrated, the negative-ion magnet was adjusted to inject mass 28 ions, and the terminal voltage was adjusted to 6.000 MV to provide $^{14}N^{3+}$ ions (from N_2^-) with precisely the same magnetic rigidity as those from C $^{14}N^-$. Increasing the terminal voltage by 6 kV (the mass of N_2 is greater than that of ^{28}Si by about one in 10^3) greatly increased the count rate of $^{28}Si^{6+}$ (to over 1 kHz). Optimizing the $^{28}Si^{6+}$ allowed us to check the terminal voltage setting and optimize the setting of the negative-ion inflection magnet (this magnet can only be set with a precision of $\sim 10^{-4}$). By gating a rate meter on the $^{14}N^{3+}$ singles, it was possible to then optimize the $^{14}N^{3+}$ rate. With the injection magnet and terminal optimized, the count rate of $^{28}Si^{6+}$ was less than 1.5 Hz, while the rate of $^{14}N^{3+}$ was $\sim$200 Hz. Electronic pile-up rejection was used, but the $^{14}N^{3+}$ count rate was maintained around 200 Hz, so that pile-up would be negligible.

The left side of Fig. 6 shows an energy spectrum, and above it a ΔE versus E spectrum obtained while injecting negative ions with a mass of 28 amu. The lowest-energy peak corresponds to $^{14}N^{3+}$ singles, while the peak at twice the energy, labeled $2\times{}^{14}N^{3+}$, results from two $^{14}N^{3+}$ ions arriving simultaneously. The coincidence peak is produced when both fragments from a single $^{14}N_2^-$ molecule are ionized to the 3+ charge state, and arrive within the 1-μs resolving time of the detector. As expected, the ΔE signal from the two ^{14}N ions is twice that from a single ^{14}N ion. The weak peak in the energy spectrum just below the 2

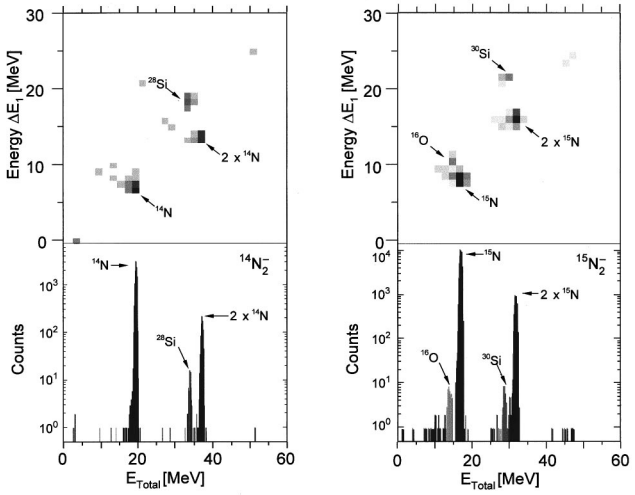

FIG. 6. Lower-left-hand figure shows an energy spectrum of 21-MeV $^{14}N^{3+}$ ions measured in our multianode ionization detector. The most intense peak at about 18 MeV corresponds to $^{14}N^{3+}$ singles arising form the dissociation of N_2^- ions in a gas stripper, while that at 36 MeV corresponds to two $^{14}N^{3+}$ ions arriving in coincidence from the dissociation of a single N_2^- ion. The peak at about 34 MeV is due to $^{28}Si^{6+}$, that has the same m/q as $^{14}N^{3+}$. The figure immediately above is the completely consistent energy loss vs energy spectrum. The spectra on the right are the analogous results obtained with a cathode containing Ti^{15}N. In each figure the data were collected in 1 min.

$\times{}^{14}N^{3+}$ is due to $^{28}Si^{6+}$; its slightly lower energy is caused by its greater energy loss in the detector's 250-μg/cm^2 mylar window. The greater rate of energy loss of the ^{28}Si in the gas is apparent in the ΔE versus E spectrum.

The observation of 1092 coincidences compared with 14 294 singles greatly exceeds the chance number of coincidences ($\sim$4; the live time was 0.94 min), and provides conclusive evidence for the existence of N_2^- molecules. Further support for their existence comes from a quantitative analysis of the spectrum. The ratio of singles to coincidences should be $2P(1-P):P^2$, where P is the probability of ionizing a nitrogen fragment formed during the breakup of a N_2^- ion to the 3+ charge state and subsequently transporting it to the detector (i.e., the transmission). Calculating P from the data in Fig. 6 yields 0.132, in excellent agreement with the measured transmission of $^{14}N^{3+}$ ions from CN^- of 13%.

Similar measurements were made with the same cathode (containing approximately equal parts of Ti ^{14}N and Ti ^{15}N) while injecting mass 30 negative ions. Since ^{30}Si and $^{15}N_2$ differ in mass by only one in 10^4, we were not able to resolve $^{15}N_2^-$ from $^{30}Si^-$ in the injector or $^{15}N^{3+}$ from $^{30}Si^{6+}$ in the high-energy beam optics. There was no difficulty in distinguishing ^{30}Si from ^{15}N or $2\times{}^{15}$N in the ionization detector, and as only $\sim$3% of Si is ^{30}Si, the count rate of ^{30}Si was less than one count per second. The results obtained when injecting mass 30 negative ions are shown on the right in Fig. 6. As in the ^{14}N case, there are peaks corresponding to $^{15}N^{3+}$ singles and twofold coincidences. Comparing the ratio of the singles to coincidences yields a slightly higher, but still reasonable, transmission of 15.1%.

The two weak peaks flanking the $1\times{}^{15}N^{3+}$ peak corre-

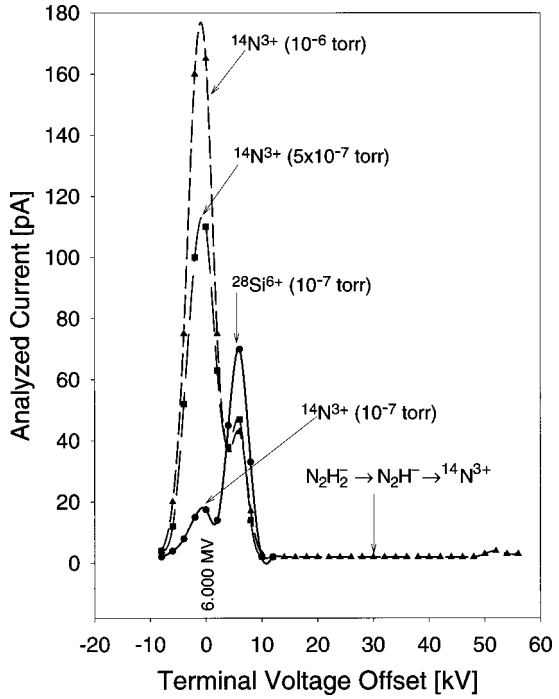

FIG. 7. Analyzed $^{14}N^{3+}$ current measured at 2-kV intervals, while the terminal voltage was raised from 5.990 to 6.060 MV. The measurements were made with a titanium cathode and various flow rates of nitrogen: the three curves correspond to zero flow (base vacuum 10^{-7} Torr), intermediate flow (5×10^{-7} Torr), and optimal flow (10^{-6} Torr). Note that the $^{28}Si^{6+}$ is resolved from the $^{14}N^{3+}$ peak, although their separation is only 6 kV. No peak was observed at 6.030 MV, where one might be expected if N_2H^- ions were being injected into the tandem.

spond to $^{16}O^{3+}$ and $^{14}N^{3+}$ that are injected as $^{14}N\,^{16}O^-$ along with other mass 30 negative ions. Neither positive ion has the right m/q to pass through the high-energy transport system, and they are therefore rigidity-selected portions of a white spectrum caused by charge-changing reactions in the accelerator. When the velocity selector (see Fig. 5) at the high-energy end of the accelerator was switched on and adjusted to pass $^{15}N^{3+}$ and other $m/q=5$ ions, these peaks were completely eliminated.

To verify further that the observed peaks were produced by nitrogen, the solid cathode was replaced with a gas cathode similar to the one developed for measuring ^{14}C on the tandem using CO_2 gas [13], and the source was supplied with N_2 gas. Two gettering materials were tried, tantalum and titanium; the latter produced much higher currents. With the entrance and exit slits of the injector opened to ±3.0 mm (the positive-ion magnet's image and object slits were left at ±0.38 mm), macroscopic $^{14}N^{3+}$ currents could be measured in the high-energy Faraday cup. Figure 7 shows the results obtained by scanning the terminal voltage in 2-kV steps from 5.990 to 6.010 MV at various nitrogen-flow rates ranging from zero to the one providing the maximum current (a range of pressures in the ion source of $10^{-7}-10^{-6}$ Torr). The maximum $^{14}N^{3+}$ current was 180 pA, which correspnds to a N_2^- current of almost 0.5 nA assuming the same transmission as measured with CN^- ions (13%). Increasing the flow rate of nitrogen gas increases the $^{14}N^{3+}$ current but decreases the $^{28}Si^{6+}$ current. At the maximum gas-flow rate the measurements were extended to 6.056 MV.

(b) Eliminating the possibility of other molecules. We have established that beams at masses 28, 29, and 30 consist of two nitrogen atoms, but how can we be sure that the nitrogen ions are not injected as low-energy tails of neighboring hydride peaks, N_2H^-? We argue against this possibility on two grounds. (1) During coincidence measurements, it was necessary to close the entrance slits to less than ±0.1 mm and the exit aperture to ±0.25 mm (the input and output slits of the high-energy positive-ion magnet were ±0.38 mm) to attenuate the negative-ion beam injected into the accelerator, so that the count rate at the ionization detector was reduced to a reasonable level. Under these circumstances, the injector resolution was better than one in 300, and the suppression of mass 29 at mass 28 was $>10^2$. Since the strength of the N_2H^- beam at mass 29 was only ~4 pA, its strength at mass 28 would be <40 fA, which is much smaller than the observed current, 500 pA. Confirmation of the suppression of the low-energy tail of the mass 29 peak was obtained by continuously tuning the injection magnet between mass 28 and mass 29, and observing the count rate of $^{14}N^{3+}$ drop to zero in between the two masses. (2) An even more convincing argument is presented in Fig. 8(a), obtained using the gas cathode. If the nitrogens we observed were injected as N_2H^-, then we would expect their count rate to peak at a terminal voltage of 6.030 MV, not 6.000 MV. Recall that the high-energy transport is set for mass 14.003 ions in the 3+ charge state with 21.019 MeV. Since N_2H^- travels to the terminal with mass 29, the terminal voltage would have to be increased by $\sim(14/28+3)/(14/29+3)=0.5\%$ to produce $^{14}N^{3+}$ ions with the same energy as those produced from N_2^- (mass=28). It is clear from Fig. 8(a) that there is no peak at 6.030 MV when the injector is set to inject mass 28. Figure 8(b) shows the results obtained when the negative-ion magnet is switched to inject ions with mass 29. The peaks at 6.000 and 6.006 MV disappear, but extremely weak peaks at 6.027 MV ($^{14}N^{3+}$) and 6.033 MV ($^{28}Si^{6+}$) are visible. The peak at 6.027 MV is partly due to the injection of $^{14}N^{15}N^-$ (nitrogen contains 0.37% ^{15}N), and partly to $^{14}N_2H^-$ ions. The $^{28}Si^{6+}$ peak is evidence for a weak beam of $^{28}SiH^-$; it cannot be $^{29}Si^-$ because $^{29}Si^{6+}$ would peak at a lower voltage (5.799 MV).

Figure 8 also provides evidence that the terminal voltage meter is calibrated correctly, and that the resolution of the high-energy transport system is as stated earlier. Figure 8(a) shows that the count rate of $^{28}Si^{6+}$ peaks at a terminal voltage 6 kV higher than $^{14}N^{3+}$. This is as it should be: the m/q of $^{28}Si^{6+}$ is one part in 10^3 lower than the m/q of $^{14}N^{3+}$, and the high-energy magnets select a constant ME/q^2. Furthermore, the Si and N peaks are resolved at full width at tenth maximum. This resolution is consistent with the stated resolution of 1/1600 full width at half maximum.

There is another means by which heavier molecular ions could be injected at mass 28, namely, molecular dissociation between the ion source and injection magnet. For example, consider $N_2H_2^-$ ions dissociating into N_2H^- and H^0. A N_2H^- ion formed in this way would have the same magnetic

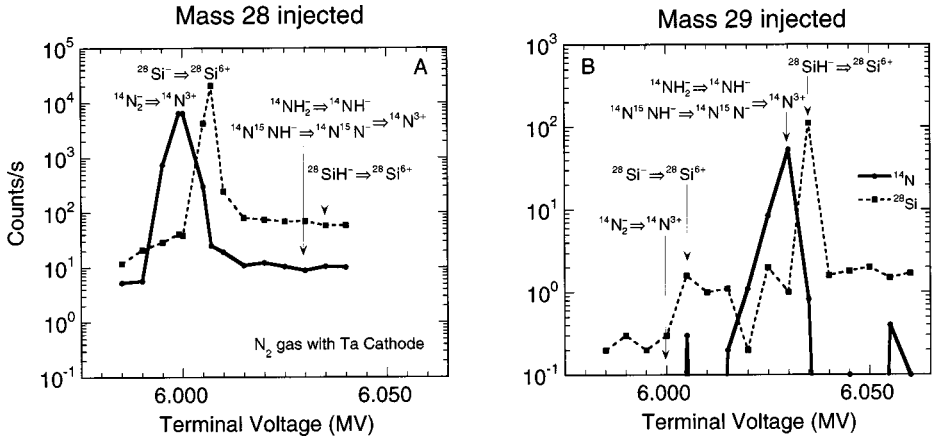

FIG. 8. (a) $^{14}N^{3+}$ and $^{28}Si^{6+}$ count rates in the gas ionization detector as the terminal voltage was raised in 5-kV intervals from 5.980 to 6.040 MV, and with the negative-ion injector set for mass 28. The solid line (with circles) is the $^{14}N^{3+}$ count rate, which peaks at a terminal voltage of 6.000 MV. The broken line (with squares) is the $^{28}Si^{6+}$ count rate measured simultaneously. The $^{28}Si^{6+}$ count rate peaks at 6.006 MV because its mass is one part in 10^3 smaller than that of N_2^-. The $^{14}N^{3+}$ and $^{28}Si^{6+}$ peaks, separated by 6 kV, are clearly resolved. No peak is observed at 6.030 MV arising from the injection of a nitrogen-containing molecule of mass 29. Therefore, neither the tail of $^{14}N_2H^-$ or $N_2H_2^- \rightarrow N_2H^- \rightarrow {}^{14}N^{3+}$ is responsible for the coincidences attributed to the break up of a $^{14}N_2^-$ ion into two $^{14}N^{3+}$ ions. (b) Similar curves while injecting mass 29 ions. Note the weak $^{14}N^{3+}$ peak at 6.030 MV due either to the injection of $^{14}N^{15}N^-$ or to $^{14}N_2H^-$. At a slightly higher energy, a weak $^{28}Si^{6+}$ peak is observed that presumably arises from the injection of $^{28}SiH^-$ ions.

rigidity as a normal ion (i.e., coming from the cathode) of mass 28.03, and therefore would be injected along with the mass 28 ions. But once again, such a N_2H^- fragment would travel to the terminal with mass 29, and the argument used above would apply—its count rate would peak in the detector at a terminal voltage of 6.030 MV, not the observed 6.000 MV. The terminal voltage argument can be used to eliminate all molecular ions that do not have mass 28. Since the detector proves that these ions are made up of two nitrogen atoms, there is only one other option other than to accept that N_2^- exists.

The measurements just described eliminate any possibility that the $^{14}N^{3+}$ ions we observe are injected into the accelerator either as a tail of a nearby molecular ion, or through the breakup of a larger molecule between the ion source and injection magnet. The only other way two nitrogens could be injected at mass 28 would be as part of a dianion of twice the mass, i.e., 56 amu. While such a possibility seems remote considering the rarity of double-negative ions, possible candidates might be N_4^{2-} and $C_2N_2H_4^{2-}$. The data presented already rule out the first possibility. If N_4^{2-} were the source of the $^{14}N^{3+}$ we observe when injecting negative ions with mass/charge ratios equal to 28, we would have seen in addition to double coincidences, triple (>200), and quadruple (~ 10) coincidences. None were seen. In principle, we could have eliminated the possibility of other dianions by looking for the atomic ions that would be produced at the terminal during their breakup, in the case of the example cited, carbon and/or hydrogen. However, to be exhaustive, we would have had to look for at least six ions (hydrogen through carbon, but not helium), or more counting their various isotopic forms. A simpler approach in principle (though not necessarily in practice) was to exploit another method that we used to study carbon dianions. The technique is called Coulomb explosion imaging (CEI) [40,41], and it provides a means of imaging the atoms that make up a molecule. In our implementation, the imaging is done in the central terminal of the accelerator. After accelerating the ions through 7.5 MV (we increased the terminal voltage to reduce multiple scattering; see below), the molecules pass through a 1.0-μg/cm^2 thick (~ 50 Å) carbon foil, where the molecular bonds are broken and the atomic fragments ionized. The atomic ions are allowed to ''Coulomb explode'' for a distance of ~ 840 μm before they are detected in a sheet of 0.25-mm-thick polycarbonate plastic,[2] manufactured to be especially sensitive to track formation (Fig. 9). About a dozen Coulomb explosion ''films'' were prepared; each was mounted on one of our standard stripper-foil frames. The tandem was opened, and the frames were loaded into the stripper-foil carousel (which has a capacity of 60 stripper-foil frames; each frame holds three foils, for a total capacity of 180 foils), the terminal was closed, and the tandem repressurized. In the carousel, the ''films'' could be lowered into and raised out of the negative-ion beam, and the carousel could be used to change from one ''film'' to another while the tandem was operating. Optimal ''exposures'' were determined using the ion chamber. Clearly the ion chamber measures the count rate of $^{14}N^{3+}$ ions, but for the CEI measurements the arrival rate of N_2^- ions at the terminal was needed. As pointed out earlier, for molecules containing two or more identical atoms, the ratio of the count rate in the singles peak to the rate in the coincidence peak can be used to determine charge-state division probabilities and the transmission through the accelerator. Dividing the count rate at the ionization detector by the calculated probability of an ion reaching the detector gave just the quantity needed. The beam was attenuated based on this calculation so that an exposure of 2 s gave a

[2]PM 355 was obtained from Pershaw Moulding Ltd., Trading Estate, Pershore, Worcestershire, England.

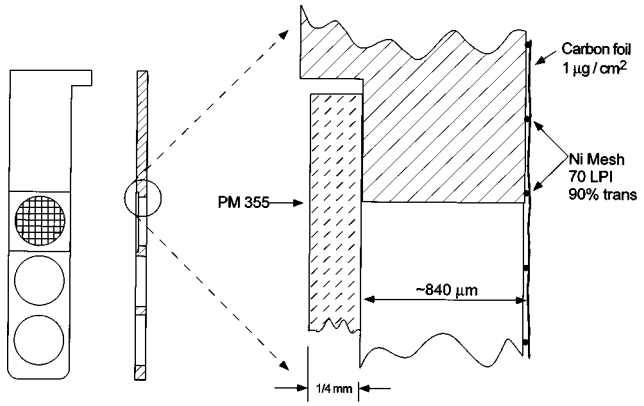

FIG. 9. On the left is one of the 60 foil holders that are loaded in a carousel in the terminal of the tandem. The holder shown has been modified by milling a recess to accommodate a 14-mm square of 0.25-mm-thick plastic track detector. Glued to the other side of the holder to support a 1-μg/cm^2 carbon foil is a piece of nickel mesh (70 lines per inch with a transmission of 90%). Details of construction are shown in the enlarged section on the right.

total of 1000 events, which over an area of 43 mm^2 gives an areal density of $\sim$25 events/mm^2.

After removal from the tandem, the track-sensitive plastic was developed in 6N NaOH for 30 min at 65 °C. The plastic was examined under a transmission microscope at 400× magnification, and photographs were taken using Kodak Tmax film. A representative photomicrograph (with scale and labels added) is shown in Figure 10. Twelve N_2^- clusters and a single track due to $^{28}Si^-$ can be seen. The plastic is sensitive enough to record tracks from H; in general, the diameter of the track increases with increasing nuclear charge. It is clear that the tracks are dominated by diatomic

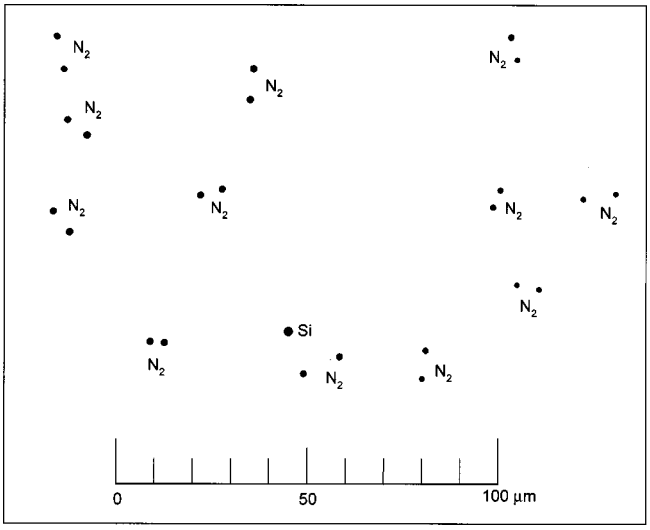

FIG. 10. A photomicrograph (one field of view, not a composite) of ^{14}N tracks produced in polycarbonate plastic (PM 355) after the 7.5-MeV N_2^- ions had passed through a 1-μg/cm^2 carbon foil placed 840 μm before the plastic. It is noteworthy that if any of the injected mass 28 ions had been, for example, $^{14}N^{12}CH_2^-$, the two protons would have been clearly visible in addition to the C and N tracks. The figure also shows a single ^{28}Si ion that is readily distinguishable by its larger diameter.

homonuclear clusters, not by triatomic or four-atom clusters, thus ruling out double-negative ions as the source of the two nitrogen ions we detect.

(c) Lifetime measurement. We obtained a lower bound for the lifetime of the longest-lived state of N_2^- using our ion-source test facility after modifying it as shown in the inset of Fig. 1. To test the performance of this arrangement, we measured the lifetime of the longest-lived state of Be^-, and obtained reasonable agreement with the accepted value (see below). Unfortunately, it is more difficult to measure the lifetimes of molecular ions than it is to measure the lifetimes of atomic ions. Molecular ions are usually (and probably always in a sputter source) produced in states of vibrational and rotational excitation that reduce the effective binding energies and probably (though not necessarily) the lifetimes of the ions. Consequently, the decay rate we determined was undoubtedly measured on some ensemble of excited states. Also, we did not produce the ions in a well-defined electronic spin state, and it is known that hyperfine states can have very different lifetimes [21,23,42]. Since we did not watch the decay of the ions through time, we could not check whether the number of N_2^- ions decreased exponentially with time as is required for the concept of ''lifetime'' to be strictly valid. Therefore, the decay rate we measured could have been fed by many states with different lifetimes. Finally, we did not determine the decay mode of the negative ion. We detected the decay by looking for the production of a neutral; we did not distinguish between autodetachment and breaking of the molecular bond to produce N^0 and N^- (the latter would decay immediately to another N^0 plus an e^-). All of these considerations imply that our measured value represents a lower limit for lifetime of the most stable state of N_2^-. So why bother with this limit? First, the observed decay of the N_2^- beam verifies that the N_2^- ion is metastable (although there can be little doubt about this). Second, the lower bound that we measure for the lifetime is fairly long, more than four times longer than the lifetime of Be^-, but half as long as the lifetime of He^- [42]. The existence of such a long-lived state of N_2^- is very surprising in light of all the theoretical expectations predicting that N_2^- is extremely short-lived. Third, a lifetime in the tens of microseconds (or longer) means that the ion exists long enough to do the sort of experiments we have already described, i.e., run it through an accelerator.

The negative-ion facility was modified by inserting a gridded lens, a drift region, and an electrostatic deflector between the ESA and the electron multiplier. The ESA was used to ''clean up'' the negative-ion beam by removing high-energy sputter tails and low-energy ions formed by molecular dissociation between the ion source and 90 ° magnet. Closing the input slits of the deflection magnet to $\pm$0.25 mm enabled us to resolve $^{28}Si^-$ from N_2^-. The ESA also removed ions that decayed between the magnet and grid of the gridded lens, which was used as the start of the decay region for the negative ions. Decay rates were determined by comparing the currents in the electron multiplier with the electrostatic deflector off and with it on. With the electrostatic deflector off, the electron multiplier measures the negative-ion current

analyzed by the deflection magnet and passing the ESA. But with the deflector on, the electron multiplier detects only uncharged atoms created between the grid of the gridded lens and the input of the electrostatic deflector (a distance of 0.71 m or a flight time of 1.93 μs for N_2^-, with an energy of 14 keV).

We checked the operation of the system by measuring the lifetime of Be^- and comparing it with the now well-established value of 45 ± 5 μs [21]. Our procedure with $^9Be^-$ was as follows: With the electrostatic deflector off, the $^9Be^-$ current was optimized in the electron multiplier (i^-). The deflector was switched on, and the ''current'' of neutral particles (we assume that the same number of electrons is produced when a 14-keV neutral enters the electron multiplier as when a negative ion with 14 keV enters it) (i^0) was measured. The lifetime is calculated from the decay rate.

$$\tau = \frac{L}{\nu}\frac{i^-}{i^0}, \tag{1}$$

where L is the distance between the grid of the einzel lens and the electrostatic deflector, and ν is the velocity of the ion. For Be we obtained $\tau=40\pm8$ μs for the autodetachment lifetime. The main uncertainties are the effective length of the drift region and contributions of other processes (such as scattering by residual gas molecules) to the neutralization rate. The vacuum in the drift region was $\sim2\times10^{-7}$ Torr. Assuming that the cross section for neutralization due to collision is of the order of 10^{-15} cm^2, the fraction of ions that suffer collision-induced neutralization in the drift region is about 5×10^{-4}. The measured fraction neutralized was $\sim2.6\times10^{-2}$, so that the background due to collision-induced neutralization is only $\sim$2% of the autodetachment rate. We checked this calculation by measuring the fraction of ions neutralized in the drift region for a number of negative ions known to be stable. The results for $^{12}C^-$, $^{13}C^-$, $^{16}O^-$, and BeO^- were 5.3×10^{-4}, 5.8×10^{-4}, 3.4×10^{-4}, and 4.6×10^{-4}, respectively. These experimental rates include the contributions from all neutralization processes including slit scattering, collision with the grid of the lens, etc.

Using N_2 gas and a Ti cathode, we set a lower bound for the lifetime of the most stable state of N_2^- at 180 ± 30 μs. The residual gas contribution to this rate was about 5%. The measured decay rate was independent of the flow rate of N_2 into the ion source over the tested pressure range of 5×10^{-7}–1.2×10^{-6} Torr (measured at the ion source) corresponding to a current range of 2.5–3.5 nA (read in the electron multiplier running with a gain of about 50). The contribution of $^{28}Si^-$ to the N_2^- current was measured by turning off the gas supply to the source. The Si and N_2 were just barely resolvable. The contribution of Si under the peak of the N_2^- peak was about 20%. Not correcting for the presence of Si^- would have increased the lower bound for the lifetime by 40%.

C. Nitrogen trimer (N_3^-)

The nitrogen trimer has been observed previously and has an electron affinity of $\sim$2.8 eV (see Illenberger *et al.* [37] for the most recent measurement of the electron affinity of N_3^-, and Zeigler and Gutsev [43] and Kaldor [44] for the state of theoretical calculations) so we anticipated little difficulty in its observation. Unfortunately, the three isotopes of silicon prevent its detection with a cathode containing a mixture of $Ti^{14}N$ and $Ti^{15}N$. No matter whether masses 42, 43, 44, or 45 are injected, positive identification of N_3^- from a measurement of current is always prevented because of one of the six combinations of $^{28,29,30}Si^{14,15}N$. Since conventional current measuring techniques could not be used, we employed the coincidence measuring method. Injecting mass 42 or 45, evidence of the existence of N_3^- can be obtained by observing two and three-fold coincidences of $^{14}N^{3+}$ and $^{15}N^{3+}$ ions, respectively.

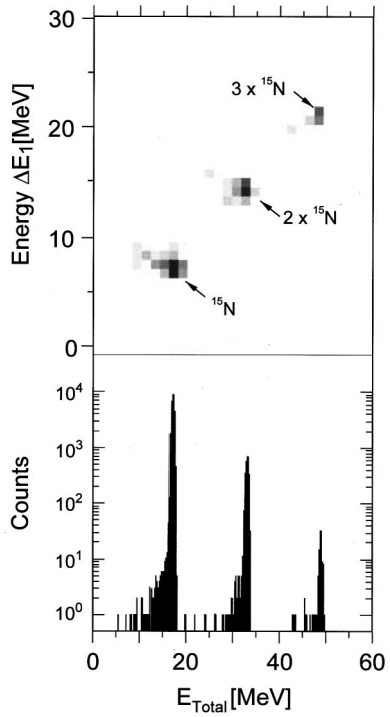

FIG. 11. Lower and upper figures show an energy spectrum and a ΔE vs E spectrum measured while injecting $^{15}N_3^-$ (mass 45) ions into the tandem. The energy spectrum shows three equally spaced peaks corresponding to the detection of one $^{15}N^{3+}$ ion, two $^{15}N^{3+}$ ions arriving in coincidence, and three $^{15}N^{3+}$ ions in coincidence; each from the dissociation of a single $^{15}N_3^-$. The ΔE vs E spectrum confirms this interpretation.

We chose to use the mass 45 negative-ion beam that contains only the weaker isotopes of silicon and nitrogen ($^{30}Si^{15}N^-$). The terminal was adjusted to 5.881 MV so that the $^{15}N^{3+}$ ions would have the same magnetic rigidity as those detected in earlier experiments, avoiding the need for any changes in the high-energy beam-transport system.

Figure 11 shows typical energy and ΔE versus E spectra. The lowest peak in the energy spectrum corresponds to the detection of single $^{15}N^{3+}$ ions, the intermediate peak to two-fold coincidences, and the highest peak to threefold events—each from the breakup of a single $^{15}N_3^-$ ion in the gas stripper. As expected, the ΔE's of the second and third peaks are multiples of the first. There is little evidence for $^{30}Si^{6+}$ in the spectrum.

Assuming that all three peaks arise from the breakup of a single $^{15}N_3^-$ molecule, their intensities should be in the ratio $3P(1-P)^2:3P^2(1-P):P^3$, where P is the probability of a

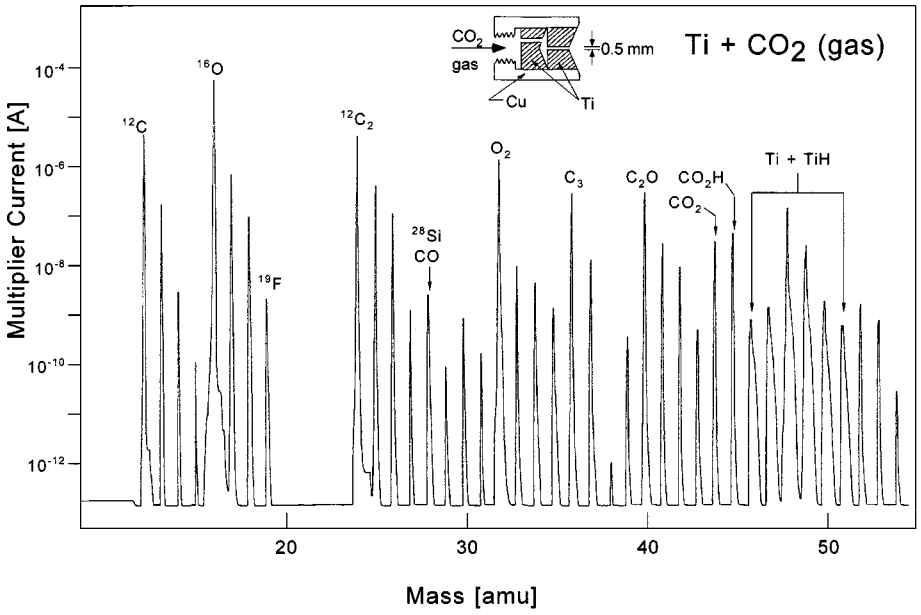

FIG. 12. Energy spectrum measured with the system shown in Fig. 1, but with a titanium gas cathode and CO_2 gas (see the inset sketch of the cathode). The purpose of the measurement was to confirm the existence of CO^- and CO_2^-. However, the identification of CO^- is difficult because the isobar ^{28}Si is a particularly prolific negative ion.

single $^{15}N^{3+}$ ion entering the detector. From the ratio of the counts we calculate 0.088 for the value of P, i.e., a transmission of 8.8%. This value is lower than calculated when accelerating N_2^-, and is a result of the reduced probability of forming 3+ ions from the lower velocity N_3^- ion.

It is difficult to determine accurately the ratio of the N_3^-/N_2^- currents because of differences in charge-state stripping efficiencies, target composition, etc. But using the transmissions we calculated from the coincidence measurements and from measurements of currents in the analyzed-beam Faraday cup, we can estimate the N_3^-/N_2^- ratio is about 1:1—an amazing factor when the electron affinities are considered (+2.8 and −2.6 eV, respectively).

D. Carbon (CO^- and CO_2^-)

In spite of many experimental and theoretical investigations, the existence and stability of CO^- and CO_2^- remain in doubt. Scheller, Compton, and Cederbaum [34] reported the electron affinities of CO and CO_2 to be −2.3 and −0.6 eV, respectively. We first attempted to detect these ions on our test facility (Fig. 1) using a cathode prepared from a mixture of powdered graphite and high-purity neodymium oxide (Nd_2O_3) tamped into a 2-mm-diameter hole in a standard copper cathode. Similar but superior results were obtained later with a titanium plus CO_2 gas cathode and a spectrum, measured using the gas cathode is shown in Fig. 12. A sectional drawing is shown in the top of the figure of the cathode designed so that the Cs^+ beam can strike only titanium, particularly in the regions of highest gas density.

In addition to the usual intense peaks from carbon at masses 12, 24, and 36 that correspond to $^{12}C^-$, $^{12}C_2^-$, and $^{12}C_3^-$, respectively, a significantly weaker peak was observed at mass 28. On the ion-source test facility there was no way of determining whether this peak was due to $^{28}Si^-$, CO^-, or a combination of both. Stronger peaks were observed at masses 40 and 45. These peaks were tentatively identified as C_2O^- and CO_2H^-, since both are known to have positive electron affinities. A comparably intense peak was also observed at mass 44, but as with the mass 28 peak its identity was uncertain; in this case we were not sure whether it was CO_2^- or $^{28}SiO^-$.

To assist with the identification of the mass 28 and 44 peaks, the gas cathode was mounted in the tandem's ion source and about 0.5 nA of mass 28 ions were injected. At a terminal voltage of 6 MV and with a tenuous gas stripper (the high-energy vacuum was 1.5×10^{-6} Torr), 0.11 nA of $^{12}C^{2+}$ ions and 0.135 nA of $^{16}O^{3+}$ ions were analyzed. If it is assumed that all of the injected beam was CO^-, then the transmissions of the C^{2+} and O^{3+} beams were 11% and 9% respectively, well within the range of expectation. The injected beam did contain a weak ^{28}Si component: 14 pA of $^{28}Si^{4+}$ was analyzed. Further confirmation that the injected beam was largely CO^- was achieved by closing off the CO_2 gas supply while analyzing the $^{12}C^{2+}$ and $^{16}O^{3+}$ beams. For both ions, the currents fell dramatically, while the analyzed $^{28}Si^{4+}$ current increased slightly. Some appreciation of the low intensity of the CO^- beam may be had by comparing its intensity (0.5 nA) with that of $^{12}C^-$ (1.7 μA) and $^{16}O^-$ (37 μA).

Similar measurements were made while injecting mass 44 ions, but because of the lower energy at the terminal, we chose to analyze both carbon and oxygen in their 2+ charge states. With 29 nA injected, 6.5 and 13.5 nA of $^{12}C^{2+}$ and $^{16}O^{2+}$ were analyzed. Assuming all 29 nA is CO_2^-, the transmission through the accelerator for C^{2+} and O^{2+} were 11.2% and 11.6%, respectively. As with the CO^-, both analyzed beams fell almost instantaneously to less than 1 nA when the CO_2 supply was valved off. A brief search for $^{28}Si^{4+}$ arising from the injection of $^{28}Si^{16}O^-$ revealed less than 20 pA. The evidence from these simple current measurements for the existence of CO^- and CO_2^- is overwhelming.

Similar measurements were made to confirm that the mass 40 peak is due to C_2O^- and that the mass 45 peak is CO_2H^-. In the latter case, not only were C^{2+} and O^{2+} analyzed, but also the protons from the hydrogen.

Although the evidence presented in the foregoing conclusively confirms the existence of CO^- and CO_2^-, we decided

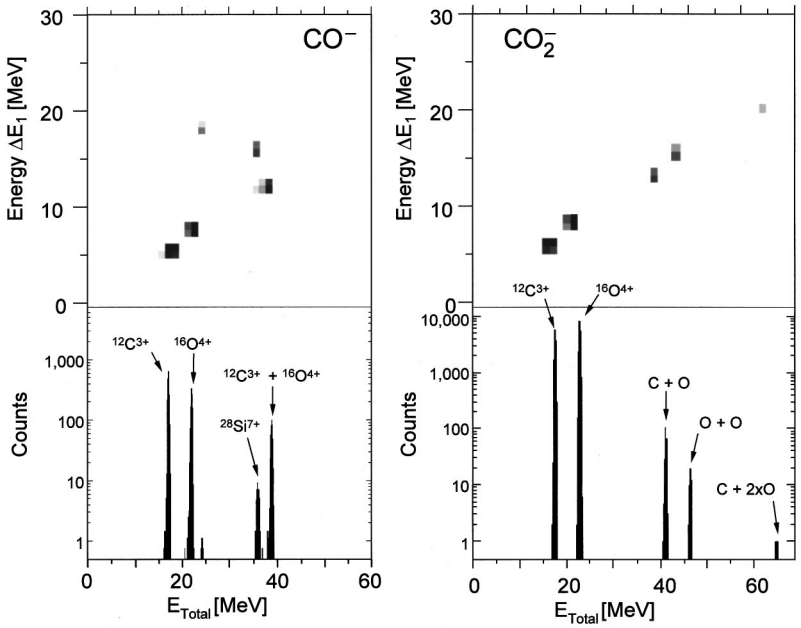

FIG. 13. Using coincidence measurements, we were able to confirm the existence of CO^- and $CO_2{}^-$. On the left are energy and energy loss vs energy spectra from the acceleration of CO^- ions. By choosing to analyze $^{12}C^{3+}$ ions, we were able to simultaneously observe $^{16}O^{4+}$ ions because both have an m/q of 4. The peaks with energies of ~16 and 22 MeV correspond to $^{12}C^{3+}$ and $^{16}O^{4+}$ ions, respectively, while the peak at 38 MeV is produced by the simultaneous arrival of a $^{12}C^{3+}$ ion and an $^{16}O^{4+}$ ion from the dissociation of a single CO^- ion at the terminal of the tandem. Note the presence of some $^{28}Si^{7+}$ that also has the same m/q. The ΔE vs E confirms the identification of the carbon and oxygen peaks. Measurements were made while injecting mass 44 ($CO_2{}^-$), and spectra are shown on the right. Here we see not only $^{12}C^{3+}$ and $^{16}O^{4+}$ single events, but also peaks due to $^{12}C^{3+}$ and $^{16}O^{4+}$ arriving in coincidence and two $^{16}O^{4+}$ in coincidence. A weak peak is also observed corresponding to a triple coincidence between $^{12}C^{3+}$ and two $^{16}O^{4+}$ ions.

to supplement it with coincidence measurements similar to those used to identify $N_2{}^-$ and $N_3{}^-$. These measurements were made with the solid cathode previously described. Because the high-energy transport system was still set up for 21-MeV $^{14}N^{3+}$ ions from CN^-, we retained the same magnetic-field values and calculated the appropriate terminal voltage to produce C^{3+} ions from CO^- with the same magnetic rigidity. We chose to analyze carbon in the 3+ charge state so that we could simultaneously analyze oxygen as $^{16}O^{4+}$ (fragments with the same m/q that result from the breakup of a molecular negative ion always have the same magnetic rigidity). Thus we were able to observe coincidences resulting from the dissociation of a single CO^- molecule.

The left side of Fig. 13 shows an energy spectrum, and immediately above it a ΔE versus E spectrum. The two most intense peaks in the energy spectrum are due to $^{12}C^{3+}$ and $^{16}O^{4+}$ single events, while the next strongest corresponds to the simultaneous arrival of both ions. Note that its energy and energy loss are equal to the sums of the energies and energy losses of the $^{12}C^{3+}$ and $^{16}O^{4+}$ single events. The weak peak just below the $^{12}C^{3+}$ and $^{16}O^{4+}$ coincidence peaks is due to $^{28}Si^{7+}$; its lower energy is due to its greater energy loss in the detector's 250-μg/cm^2 mylar window.

Similar measurements were made while injecting mass 44 ions into the tandem. The right-hand side of Fig. 13 shows the resulting energy and energy loss versus energy spectra. The terminal voltage was chosen such that $^{12}C^{3+}$ and $^{16}O^{4+}$ had the same magnetic rigidity as the ions studied previously. In addition to the peaks corresponding to the $^{12}C^{3+}$ and $^{16}O^{4+}$ singles, we were able to observe the simultaneous arrival of $^{12}C^{3+}$ and $^{16}O^{4+}$, two $^{16}O^{4+}$ ions, and a $^{12}C^{3+}$ with two $^{16}O^{4+}$ ions, each originating from the dissociation of a single $CO_2{}^-$ molecule. Note that the relative number of coincidences were less than in the CO^- case because the lower energy of the $CO_2{}^-$ constituents at the terminal reduced the probabilities of forming C^{3+} and O^{4+} ions.

We followed up the measurements on the accelerator with lifetime measurements on the modified ion-source test facility. The values we obtained are 140 μs for CO^- and 170 μs for $CO_2{}^-$. Because the mass difference between CO and Si is only 60% of the mass difference between N_2 and Si, the lifetime measurements were more difficult than they were for $N_2{}^-$. Because we were unable to resolve CO^- from $^{28}Si^-$ or $^{28}SiO^-$ from $CO_2{}^-$, the measured ratios of i^-/i^0 were larger than they should have been, causing us to overestimate the stability of the negative ion. The difficulties related to measuring the lifetimes of molecular ions tend to make measured lifetimes shorter than the lifetime of the longest-lived state (see comments in Sec. III B 2 *c*). Therefore, it is not immediately clear whether the values we obtained are likely to be too long or too short. As far as we are aware, there are no lifetime measurements for CO^- (due, no doubt, to the fact that most people have believed that it is impossible to form). There is only one previous measurement by Compton [45] of the lifetime of $CO_2{}^-$. His result was 90 ± 20 μs.

IV. DISCUSSION

The present work was undertaken to demonstrate that cesium sputter sources, particularly those outfitted with spherical ionizers, can produce moderately intense beams of meta-

stable negative ions. The highly focused Cs^+ beams in such sources create deep, small-diameter, sputter craters that frequently contain dense plasma balls. Presumably conditions in these plasmas are similar to the conditions in alkali-vapor charge-exchange canals. The major difference is that the charge-changing collisions in the plasma regions in sputter sources occur at energies of a few eV rather than a few keV typical in adder canals. Most cross sections for electron transfer peak in the range of a few keV, suggesting that charge-exchange sources should produce metastable ions more efficiently than sputter sources. However, the interaction time between the plasma and the neutral atom is undoubtedly longer in the sputter source, and the longer interaction time may compensate for the difference in cross section. In fact, in the sputter source, atoms are only efficiently removed from the plasma after they obtain a negative charge, at which point they can be extracted by the electric field present at the face of the cathode. Neutral atoms escape only by diffusion, and positive ions are trapped inside the plasma. So from the theoretical standpoint, there is no *a priori* reason why Cs-sputter sources should not produce metastable ions with currents comparable to those obtained using charge exchange.

As noted in Sec. I, there have not been many experimental studies of the formation of metastable ions in sputter sources. From a theoretical and experimental standpoint, the most thoroughly studied metastable atomic negative ions are He^- and Be^- but other atomic metastable ions are known including Mg, Zn, Cd, and Hg, and probably several of the rare earths. Sputter sources produce only low currents of He^-, but, as argued in Sec. I, these low yields are probably because of the low chemical reactivity of He and not to an inherent inability of sputter sources to form metastable ions. On the other hand, sputter sources can produce currents on the order of a microamp of Be^-; these currents are comparable to the currents obtainable using charge-exchange sources.

Our knowledge of metastable molecular ions is even more primitive. Calculations of the stability of negative ions is difficult because adding an electron to a neutral atom changes the total electronic energy of the system by about one part in ten thousand, and calculating molecular energies to this precision is at or beyond the current state of the art. Determining experimentally that an ion is metastable usually requires measuring the ion's lifetime. Using in-beam techniques, these measurements are difficult and limited to a range of ~ 0.1–100 μs. New techniques using storage rings and photodetachment methods have extended these measurements to much longer (~ 1 ms) and shorter (~ 10 ps) lifetimes. For some ions, low-energy electron-scattering data can be used to rule out the existence of bound negative-ion states built on the ground-state atom, while resonances at a few eV are taken as evidence of the formation of metastable negative ions built on excited states. Determining reliably the lifetimes of these states from the scattering data is often difficult, so frequently it is impossible to determine whether such resonances imply the existence of metastable ions that one can actually produce in an ion source and study with a mass spectrometer where the transport times are on the order of a microsecond.

Intrigued by the negative-ion stability diagram (Fig. 1A) in Ref. [34], we decided to examine the two ions, N_2 and CO, with the smallest electron affinities (-2.7 and -2.3 eV). In both cases, we have been able to measure macroscopic beams of the negative and positive ions formed after stripping in the accelerator. A significant experimental difficulty in studying N_2^- and CO_2^- is the presence of $^{28}Si^-$ at mass 28. We eliminated any possible confusion with Si or other ion of mass 28 by injecting the mass 28 beam into the tandem, and using our gas-ionization detector to identify the positive-ion components produced during molecular destruction and stripping at the terminal. Using our modified ion-source test facility, we were able to make in-beam measurements of the lifetimes of these ions, and found that they were on the order of 150 μs. Consequently, despite the large negative electron affinities of the nitrogen dimer and carbon monoxide, the metastable negative ions of these molecules are comparatively long lived and can be formed in a sputter source with currents ranging from hundreds of pA to about 1 nA.

We also report results of studies with N_3^- and CO_2^-. Despite the much larger electron affinities of these molecules (~ 2.8 eV for N_3^-, which is actually bound; and -0.6 eV for CO_2^-), the currents of these negative ions were comparable to those we obtained for N_2^- and CO^-. It therefore appears that neither the binding energy nor the lifetime of a molecular negative ion is a good predictor of the size of the negative ion current that can be produced in a sputter source.

ACKNOWLEDGMENTS

The authors' thanks are due to Harry White for maintaining the ion sources and operating our tandem single handedly. We would like to thank Ted Litherland, whose suggestion was the initial catalysis for this paper, and whose devil's advocacy helped us to argue more persuasively for the existence of N_2^- and CO_2^-. We are also grateful to the NSF for their support (Grant No. Phys 9417364), which made this work possible.

[1] *Atomic Energy Levels*, edited by C. A. Moore, Natl. Bur. Stand. U.S. Circ. No. 467 (U.S. GPO, Washington, DC, 1949).

[2] W. R. Bozman, C. H. Corliss, W. F. Meggers, and R. E. Trees, J. Res. Natl. Bur. Stand. **50**, 131 (1953).

[3] C. Y. Tang, J. R. Wood, D. J. Pegg, J. Dellwo, and G. D. Alton, Phys. Rev. A **48**, 1983 (1993).

[4] P. Kristensen, U. V. Pedersen, V. V. Petrunin, T. Andersen, and K. T. Chung, Phys. Rev. A **55**, 978 (1997).

[5] J.-J. Hsu and K. T. Chung, Phys. Rev. A **52**, R898 (1995).

[6] P. Kristensen, V. V. Petrunin, H. H. Andersen, and T. Andersen, Phys. Rev. A **52**, R2508 (1995).

[7] C. A. Nicolaides and G. Aspromallis, J. Phys. B **19**, L841 (1986).

[8] C. A. Nicolaides and G. Aspromallis, J. Phys. B **16**, L251 (1983).

[9] W. Kutschera, D. Frekers, R. Pardo, K. E. Rehm, R. K.

Smither, and J. L. Yntema, Nucl. Instrum. Methods Phys. Res. A **220**, 118 (1984).
[10] R. Middleton (unpublished).
[11] R. Middleton, Nucl. Instrum. Methods Phys. Res. **214**, 139 (1983).
[12] R. Middleton and J. Klein (unpublished).
[13] R. Middleton, J. Klein, and D. Fink, Nucl. Instrum. Methods Phys. Res. B **43**, 231 (1989).
[14] R. Middleton and J. Klein, Nucl. Instrum. Methods Phys. Res. B **123**, 532 (1997).
[15] R. Middleton and J. Klein, Phys. Rev. A **60**, 3535 (1999).
[16] K. Bethge, E. Heinicke, and H. Baumann, Phys. Lett. **23**, 542 (1966).
[17] A. W. Weiss, Phys. Rev. Lett. **166**, 70 (1968).
[18] T. J. Kvale, G. D. Alton, R. N. Compton, D. J. Pegg, and J. S. Thompson, Phys. Rev. Lett. **55**, 484 (1985).
[19] C. F. Bunge, M. Galán, R. Jáuregui, and A. V. Bunge, Nucl. Instrum. Methods Phys. Res. **202**, 299 (1982).
[20] D. R. Beck and C. A. Nicolaides, Int. J. Quantum Chem. **18**, 467 (1984).
[21] P. Balling, L. H. Andersen, T. Andersen, H. K. Haugen, P. Hvelplund, and K. Taulbjerg, Phys. Rev. Lett. **69**, 1042 (1992).
[22] T. Brage and C. Froese Fischer, Phys. Rev. A **44**, 72 (1991).
[23] H. H. Andersen, P. Balling, V. V. Petrunin, and T. Andersen, J. Phys. B **29**, L415 (1996).
[24] G. Aspromallis, C. Sinanis, and C. A. Nicolaides, J. Phys. B **29**, L1 (1996).
[25] G. Aspromallis, C. A. Nicolaides, and D. R. Beck, J. Phys. B **19**, 1713 (1986).
[26] H. F. Schaefer, R. A. Klemm, and F. E. Harris, J. Chem. Phys. **51**, 4643 (1969).
[27] L. D. Thomas and R. K. Nesbet, Phys. Rev. A **12**, 2369 (1975).
[28] H. Müller, D. Gador, F. Wiegershaus, and V. Kempter, J. Phys. B **29**, 715 (1996).
[29] H. Hiraoka, R. K. Nesbet, and L. W. J. Welsh, Phys. Rev. Lett. **39**, 130 (1977).
[30] O. Heber, I. Gertner, I. Ben-Itzhak, and B. Rosner, Phys. Rev. A **38**, 4504 (1988).
[31] Y. K. Bae, M. J. Coggiola, and J. R. Peterson, Phys. Rev. A **29**, 2888 (1984).
[32] H. S. W. Massey, *Negative Ions* (Cambridge University Press, London, 1976).
[33] F. R. Gilmore, J. Quant. Spectrosc. Radiat. Transf. **5**, 369 (1965).
[34] M. K. Scheller, R. N. Compton, and L. S. Cederbaum, Science **270**, 1160 (1995).
[35] J. L. Franklin, V. H. Dibeler, and R. M. Reese, J. Am. Chem. Soc. **80**, 298 (1958).
[36] R. L. Jackson, M. J. Pellerite, and J. I. Brauman, J. Am. Chem. Soc. **103**, (1981).
[37] E. Illenberger, P. B. Comita, J. I. Brauman, H-P. Fenzlaff, M. Heni, N. Heinrich, W. Koch, and G. Frenking, Ber. Bunsenges. Phys. Chem. **89**, 1026 (1985).
[38] C. L. Bennett, R. P. Beukens, M. R. Clover, H. E. Gover, and R. B. Liebert, Science **198**, 508 (1977).
[39] D. Fink, R. Middleton, J. Klein, and P. Sharma, Nucl. Instrum. Methods Phys. Res. B **47**, 79 (1990).
[40] Z. Vager, E. P. Kanter, G. Both, P. J. Coonery, A. Faibis, W. Koenig, B. J. Zabransky, and D. Zajfman, Phys. Rev. Lett. **57**, 2793 (1986).
[41] D. S. Gemmell, Chem. Rev. **80**, 301 (1980).
[42] T. Andersen, L. H. Andersen, P. Balling, H. K. Haugen, W. W. Smith, and K. Taulbjerg, Phys. Rev. A **47**, 890 (1993).
[43] T. Ziegler and G. L. Gutsev, J. Comput. Chem. **13**, 70 (1992).
[44] U. Kaldor, Int. J. Quantum Chem., Symp. **24**, 291 (1990).
[45] R. N. Compton, P. W. Reinhardt, and C. D. Cooper, J. Chem. Phys. **63**, 3821 (1975).